Physical Oceanography Distributed Active Archive Center (PO.DAAC)

CYGNSS Level 2 Heat Flux Dataset Climate Data Record Version 1.0 Guide Document

6 October 2020

Version 1.0

Document Clearance Number: 20-4363

Jet Propulsion Laboratory
Pasadena, California

TABLE OF CONTENTS

VERSION 1.0 ..... **1**

1. ABSTRACT: **2**
2. ACKNOWLEDGEMENTS: **3**
3. MISSION DESCRIPTION: **3**
3.1 MISSION REQUIREMENTS 4
3.2 SATELLITE DESCRIPTION **5**
4. SENSOR OVERVIEW: **6**
4.1 PRINCIPLES OF OPERATION **6**
5. PROCESSING METHODOLOGY: **10**
6. CALIBRATION AND VALIDATION: **12**
7. DATASET DESCRIPTION: **13**
7.2 VARIABLE TYPES 14
7.3 BIT BY BIT DESCRIPTION OF QUALITY FLAG VARIABLE 18
7.4 GRID DESCRIPTION 18
7.5 RELATED PRODUCTS 19
8. DATA ACCESS: **19**
OBTAINING DATA AND DOCUMENTATION: 19
CONTACT INFORMATION: 20
9. READ SOFTWARE: **20**
10. REFERENCES: **20**
11. ACRONYMS: **22**
12. DOCUMENT HISTORY **22**
DOCUMENT LAST MODIFIED DRAFT DATE: 22
DOCUMENT REVIEW DATE: 23
CITATION: 23
DOCUMENT LOCATION: 23

1. Abstract:

This ocean surface heat flux dataset is provided as a service to the oceanographic and meteorological research communities on behalf of a NASA ROSES funded project within CYGNSS Science Team in direct collaboration with the CYGNSS Mission. This document details the CYGNSS Level 2 Climate Data Record Version 1 dataset which provides data on CYGNSS specular points on a nominal 25 km diameter footprint in daily netCDF-4 files. Development and distribution of this dataset is made possible through funding provided by NASA.

2. Acknowledgements:

NOTE: Please refer all questions concerning this dataset to PO.DAAC User Services: podaac@podaac.jpl.nasa.gov.

A significant portion of the research for this document was carried out at the Jet Propulsion Laboratory, California Institute of Technology, under a contract with the National Aeronautics and Space Administration. The following people have contributed to the procurement of this dataset and user guide documentation:

Principal Investigator:
Dr. Derek Posselt[1]

Co-Investigators:
Dr. Juan Crespo[1]

User Guide Authors:
David Moroni[1]
Juan Crespo[1]
Derek Posselt[1]

User Guide Content Reviewers/Contributors:
Chris Ruf[2]

[1]Jet Propulsion Laboratory, California Institute of Technology
[2]University of Michigan

3. Mission Description:

The Cyclone Global Navigation Satellite System (CYGNSS), launched on 15 December 2016, is a NASA Earth System Science Pathfinder Mission that was launched with the purpose to collect the first frequent space-based measurements of surface wind speeds in the inner core of tropical cyclones. Made up of a constellation of eight micro-satellites, the observatories provide nearly gap-free Earth coverage using an orbital inclination of approximately 35° from the equator, with a mean (i.e., average) revisit time of seven hours and a median revisit time of three hours. This inclination allows CYGNSS to measure ocean surface winds between approximately 38° N and 38° S latitude. This range includes the critical latitude band for tropical cyclone formation and movement.

CYGNSS has the capability to measure the ocean surface wind field with unprecedented temporal resolution and spatial coverage, under all precipitating conditions, and over the full dynamic range of wind speeds experienced in a tropical cyclone. This mission uses an innovative combination of all-weather performance Global Positioning System (GPS) ocean surface reflectometry with the sampling properties of a dense constellation of eight observatories.

What makes CYGNSS unique is that it is NASA's first mission to perform surface remote sensing using an existing Global Navigation Satellite System (GNSS)— a satellite constellation that is used to pinpoint the geographic location of a user's receiver anywhere in the world. A number of GNSS systems are currently in operation, including: the United States' Global Positioning System (GPS), the European Galileo, the Russian Federation's Global Orbiting Navigation Satellite System (GLONASS), and the Chinese Beidou. CYGNSS has opted to use only the United States' GPS constellation.

Unlike radar scatterometers (e.g., ISS-RapidScat, QuikSCAT, and ASCAT) that both emit microwave radar pulses and receive their backscattered signals, CYGNSS functions as a constellation of passive sensors that receive the signal of surface-reflected GPS pulses. One of the most well-known limitations of traditional microwave scatterometry (particularly, Ku-band) is signal degradation of the microwave pulses when passing through intense rainfall as typically observed within hurricane eyewalls, thus limiting its utility in retrieving observations of high wind speeds in this critical region of the storm. Reflected GPS signals, on the other hand, operate at a much lower microwave frequency utilized by the GPS constellation that is able to penetrate thick clouds and precipitation around the eyewall and provide the first opportunity to remotely measure inner-core wind speeds.

The goal of the mission is to study the relationship between ocean surface properties (i.e., surface wind speed), moist atmospheric thermodynamics, heat transfer, and convective dynamics in the inner core of a tropical cyclone. This will allow scientists to determine how a tropical cyclone forms, whether or not it will strengthen, and if so by how much. The successful completion of these goals will allow the mission to contribute to the advancement of tropical cyclone forecasting and tracking methods.

3.1 Mission Requirements

A summary of the original CYGNSS Baseline Science requirements is given in Table 1, followed by the CYGNSS Threshold Science requirements provided by Table 2.

Quantity	Requirement	Applicable Range
Wind speed		3-70 m/s

Field of View	5x5 km	Specular Point
Spatial resolution	25x25 km	DDMs
Mean Revisit Time	12 hours	24-hour time window
Coverage	70% of all tropical cyclone tracks between 35 deg. South and 35 deg. North latitude	24-hour time window
Mission duration	24 months	Prime Mission

Table 1: CYGNSS Baseline Science Requirements

Quantity	**Requirement**	**Applicable Range**
Wind speed	2 m/s or 10% RMS error	3-40 m/s
Field of View	5x5 km	Specular Point
Spatial resolution	50x50 km	DDMs
Temporal Sampling	Less than 12 hours	24-hour time window
Coverage	60% of all tropical cyclone tracks between 35 deg. South and 35 deg. North latitude	24-hour time window

Table 2: CYGNSS Threshold Science Requirements

3.2 Satellite Description

CYGNSS consists of a constellation of 8 individual small satellites, also commonly referred to as observatories. Attitude is 3-axis stabilized with 2.1° (3σ) knowledge and 2.8° (3σ) control using horizon sensors, a magnetometer, pitch momentum wheel, and torque rods. Observatory mass and power are estimated to be ~25 kg and ~38 watts. Table 3 details the nominal orbit parameters of each spacecraft.

Orbital Period	95 minutes
Orbit Type	Low-Earth Asynchronous
Mean Altitude above Equator	525 km
Inclination	35^{o}

Table 3: Nominal Orbit Parameters

4. Sensor Overview:

Each CYGNSS Observatory includes a Delay Doppler Mapping Instrument consisting of a multi-channel GPS receiver, low gain zenith antennas and high gain nadir antenna. Figure 1 below illustrates each sensor.

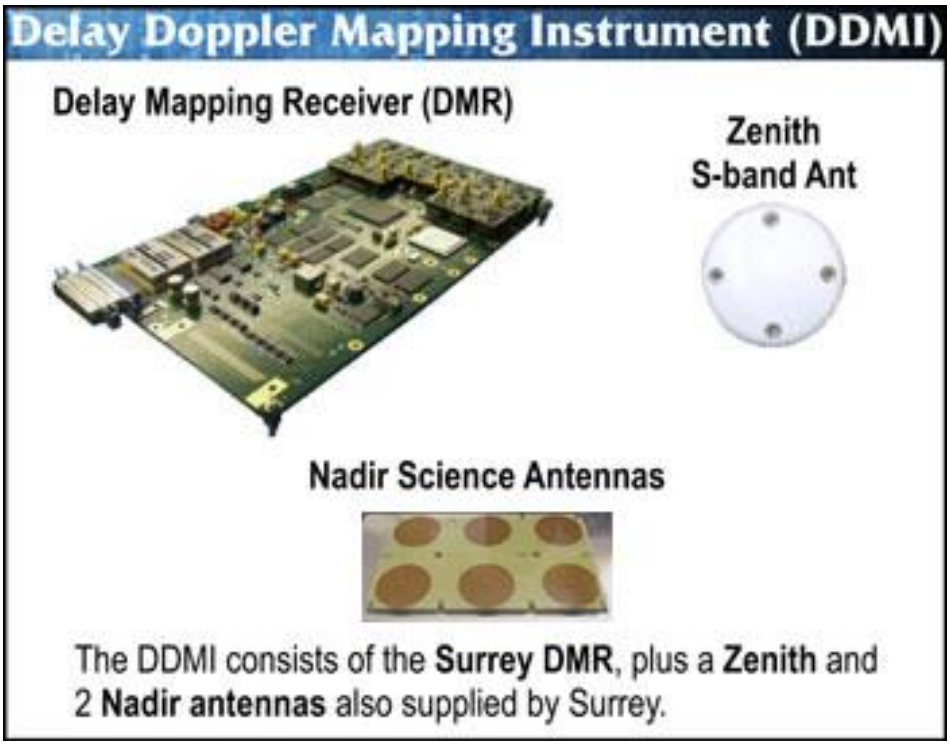

Figure 1: CYGNSS Sensor Illustration.

4.1 Principles of Operation

Each CYGNSS observatory contains a delay Doppler mapping instrument (DDMI), which receives direct signals from GPS satellites as well as signals reflected off the ocean surface. The direct signals pinpoint the location of the observatory, while the reflected signals respond to ocean surface roughness, from which wind speed is derived. Signals are measured at 1Hz, and each of the 8 observatories is capable of measuring 4 simultaneous reflections, resulting in 32 wind measurements per second around the globe. This provides the ability to measure ocean surface winds with unprecedented temporal resolution and spatial coverage under all precipitating conditions, up to and including those experienced in the hurricane eyewall.

Figure 2 illustrates the propagation and scattering geometries associated with the GPS bistatic radar approach to ocean surface scatterometry. The direct GPS signal provides a coherent reference for the coded GPS transmitted signal. It is received by a right-hand circularly polarized (RHCP) receive antenna on the zenith side of the spacecraft. The quasi-specular, forward-scattered signal from the

ocean surface is received by a downward-looking left-hand circularly polarized (LHCP) antenna on the nadir side of the spacecraft. The properties of the scattered signal are sensitive to the sea surface roughness, from which local wind speed can be derived (Zavorotny & Voronovich, 2000).

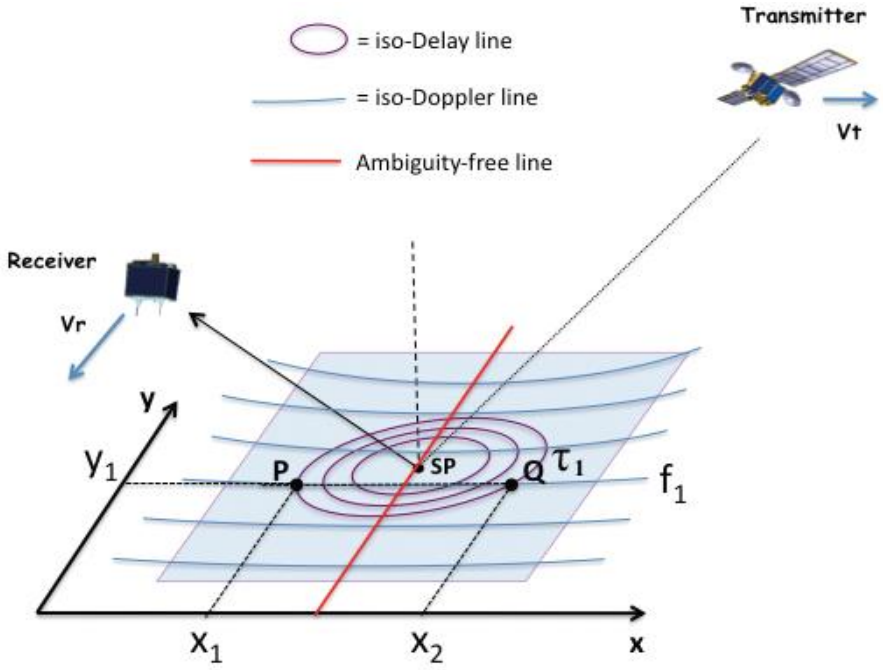

Figure 2: GPS signal propagation and scattering geometries for ocean surface bistatic quasi-specular scatterometry. Reused from Clarizia & Ruf (2016), © 2016 IEEE.

The scattering cross-section image produced by CYGNSS mission is shown in Figure 3. Variable lag correlation and Doppler shift, the two coordinates of the image, enable the spatial distribution of the scattering cross section to be resolved (Gleason et al., 2005). This type of scattering image is referred to as a delay Doppler map (DDM). Estimation of the ocean surface roughness and wind speed is possible from two properties of the DDM. The maximum scattering cross section (the dark red region in Figure 3) is related to roughness and therefore wind speed. This requires power calibration of the DDM. Wind speed can also be estimated from the shape of the scattering cross section pattern in the DDM (the red and yellow regions in Figure 3). The pattern is produced by scattering from an area surrounding the nominal specular point (SP) on the surface. For a smooth, mirror-like surface, the pattern would be defined by the GPS bistatic radar ambiguity function. But as the surface becomes rougher, the GPS signal is scattered by a larger area of the surface and into many directions. This causes a reduction in the maximum cross section near the SP and the “spreading” of power into wider delay/ Doppler bins. The shape of the DDM pattern also contains information about the sea surface winds. In particular, the shape of its dependence on delay is sensitive to the significant wave height of the sea surface, which is correlated with wind speed.

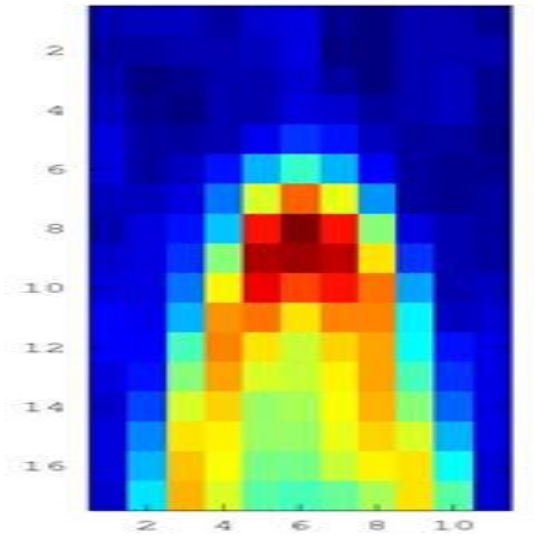

Figure 3: Spatial distribution (in delay and Doppler coordinates) of the ocean surface scattering measured by CYGNSS, referred to as the delay Doppler map, or DDM (image credit: Dr. Chris Ruf, University of Michigan, 2019).

CYGNSS measures the power in the GPS signal scattered by the ocean surface after the signal is selectively filtered by time delay and Doppler shift to create a DDM. The time delay is the difference in time of arrival between the direct signal (propagating directly from the GPS satellite to the CYGNSS satellite) and the signal scattered by the ocean surface. The Doppler shift is the difference in frequency between the received direct signal and the received ocean-scattered signal. Both delay and Doppler are varied in the DDM across a range that includes the nominal SP on the surface. Shorter delays correspond to locations above the surface, from which there is no significant scattered signal. Longer delays can be mapped to iso-delay contours on the surface surrounding the SP. Varying Doppler of the scattered signals can also be mapped to iso-Doppler contours on the surface that intersect the delay contours to create the DDM. The DDM is thus a map of the diffuse surface scattering in the vicinity of the nominal SP. The transformation between spatial location on the sea surface and location in the DDM is one to one at the DDM specular location but can have ambiguities outside the specular region (i.e., multiple spatial locations mapped to the same DDM location).

CYGNSS spatial sampling produces Level 2 wind speed data products, which consist of 32 simultaneous single pixel “swaths” that are 25 km wide and typically hundreds of kilometers long, as the SPs move across the surface due to orbital motion by CYGNSS and the GPS satellites. Examples of the spatial coverage obtained after 90 minutes (one orbit) and 24 hours are shown in Figure 4a–b. Temporal and spatial sampling occurs randomly due to the asynchronous nature of the CYGNSS and GPS satellite orbits. As a result, the CYGNSS revisit time is best described by its probability distribution. The distribution, shown in Figure 4c, is derived empirically using a mission simulator to determine the time and location of each sample within the ± 38º latitude coverage zone and then examining the time difference between samples at the same location. The empirical distribution features a high probability of very short revisit times (resulting from sequential samples by trailing satellites spaced dozens of minutes apart) and a long, tapering “tail” at higher revisit times. Its median value is 3 hours, and the mean revisit time is 7 hours.

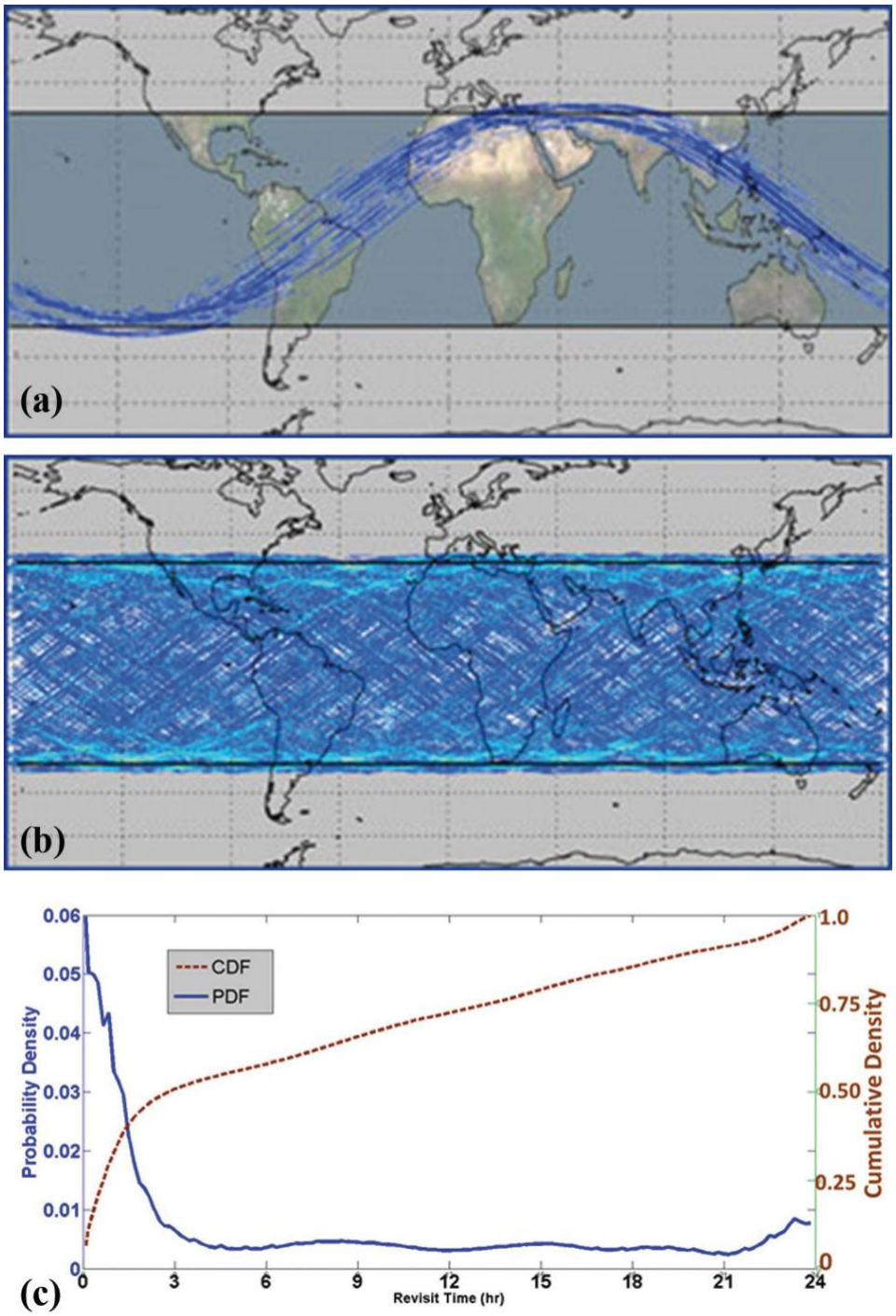

Figure 4: CYGNSS coverage illustration. Each low-Earth orbiting CYGNSS observatory will orbit at an inclination of 35º and is capable of measuring four simultaneous reflections, resulting in 32 wind measurements per second across the Earth. The configuration is optimized for high temporal resolution wind fi eld imagery of TC genesis, intensifi cation, and decay. Shown here are the CYGNSS spatial coverage tracks after (a) 90 minutes and (b) 24 hours. Temporal sampling is characterized by the probability and cumulative density functions of revisit time, shown in (c). Sampling occurs randomly due to the asynchronous nature of the CYGNSS and GPS satellite orbits, and revisit time is best characterized via statistics of these distributions. The median and mean revisit times are, respectively, 3 and 7 hours.

5. Processing Methodology:

The Coupled Ocean-Atmosphere Response Experiment (COARE) algorithm (Edson et al. 2013) is a widely used parameterization to estimate latent and sensible fluxes and their respective transfer coefficients. The COARE bulk flux algorithm is based on the Monin-Obukhov similarity theory (MOST; Fairall et al. 1996 & 1997) and has been widely used to estimate surface heat fluxes over the open oceans. While COARE's initial intentions were for low to moderate wind speeds, the version used for this product, COARE 3.5, has been verified with direct in-situ flux measurements for wind speeds up to 25 m/s.

COARE 3.5 utilizes the bulk aerodynamic formulas in order to estimate latent (LHF) and sensible (SHF) heat fluxes, which are as follows:

$$LHF = \rho_a L_v C_{DE} U(q_s - q_a) \quad (1)$$

$$SHF = \rho_a c_p C_{DH} U(T_s - T_a) \quad (2)$$

Here, ρ_a is the air density at the surface [kg m^{-3}]; L_v is the latent heat of condensation (2.5x10^6 J kg^{-1}); and c_p is specific heat at constant pressure (1004 J K^{-1} kg^{-1}). C_{DE} and C_{DH} are, respectively, the exchange coefficients of moisture and sensible heat [unitless]; U is the surface winds [m s^{-1}], T_s and q_s are temperature [K] and specific humidity [kg kg^{-1}], respectively, at the surface, while T_a and q_a are the same but at 10 meters above the surface.

Since CYGNSS does not provide temperature, humidity, surface pressure or density, we obtain these values from the NASA Modern-Era Retrospective Analysis for Research and Applications, Version 2 (MERRA-2; Gelaro et al. 2017). MERRA-2 uses data assimilation to combine all available in-situ and satellite observation data with an initial estimate of the atmospheric state, provided by a global atmospheric model. Variables required for the surface heat flux estimates are available with a temporal resolution of one hour and a spatial resolution of 0.5°x0.625°.

COARE 3.5 parameterizes the drag coefficients (C_{DE} and C_{DH}) in the bulk formulas (Eqns. 1 & 2) as a function of gustiness, surface roughness, and atmospheric stability; it is mathematically expressed as:

$$C_D(z/z_o, z/L, G) = \frac{-\overline{uw}}{U_r S_r} = \frac{-\overline{uw}}{U_r^2 G} = \left[\frac{\kappa}{\ln(z/z_o) - \psi_m(z/L)}\right]^2 \quad (3)$$

Here, z is the height above the surface [m]; κ is the von Kármán constant (set to a value of 0.4; unitless); z_o is the aerodynamic roughness length [m], and ψ_m is a dimensionless function that accounts for the effects of atmospheric stratification. G is the gustiness parameter, defined as the ratio of the wind speed, S_r [m s^{-1}], to the vector-averaged wind, U_r [m s^{-1}] (Beljaars and Holslag 1991; Edson et al. 2013). This parameterization attempts to account for mass, momentum, and heat

transfer at lower wind speeds, but is non-zero because of the gustiness. This results in shear-driven turbulence produced by gusts that significantly drive exchanges in convective conditions (Fairall et al. 1996, Edson et al. 2013).

In order to use MERRA-2 data at each CYGNSS specular point, the nearest MERRA-2 grid point needs to be matched in time and space. Since MERRA-2 features an hourly temporal resolution and 0.5°x0.625° spatial resolution, we use a tri-linear interpolation method to match the CYGNSS and MERRA-2 data. The inputs from MERRA-2 include temperature and humidity (at the surface and 10-meters) and air density.

For surface winds, two wind speed products are used from CYGNSS's L2 wind speed product: the minimum variance of the fully developed seas (FDS) wind speed and young seas with limit fetch (YSLF) wind speeds. In order to maintain consistency for the data users analyzing surface fluxes and wind speeds from CYGNSS, LHF and SHF are calculated throughout the whole mission using both wind speed products. While it is ultimately up to the users to decide when it is best to use FDS and YSLF products, it is generally recommended that the FDS products are used for most applications and analysis, while the YSLF product should be utilized for higher wind situations, rapidly developing systems, and strong curvature in the flow (i.e. tropical and extratropical cyclones).

Given that COARE 3.5 is validated for wind speeds up to 25 m/s, LHF and SHF estimates are flagged when wind speeds surpass this limit. When wind speeds exceed 25 m/s, sea spray ejected from the ocean surface have a non-negligible effect on the air-sea heat fluxes (Richter and Stern 2014). Additionally, estimates of the drag coefficient breakdown above this threshold; these result in the LHF and SHF estimates becoming increasingly erroneous.

Additional quality flags are produced for range corrected gain (RCG) less than 3 due to unreliability in wind speeds.

Inputs from every CYGNSS specular point and matched MERRA-2 data are inserted into the COARE 3.5 algorithm to estimate latent and sensible heat fluxes. COARE produces a first guess of the surface heat fluxes and uses this guess to initialize a stability iteration loop. Within this loop, COARE computes the Monin-Obukhov length, roughness length, and transfer coefficients along with a stability dependence. For the initial version of the Surface Heat Flux Product, the loop is repeated 10 times as various trials have shown that this is the minimum needed for the values to each an asymptote at each specular point. Future versions of this product may alter the loop so it automatically terminates when the values converge.

The transfer coefficients calculated within the loop are used to estimate LHF and SHF using the bulk aerodynamic formulas (Eqns. 1 & 2), combined with both wind speed products from CYGNSS and the thermodynamic variables from MERRA-2.

This results in two products each for LHF and SHF (Crespo et al. 2019), which are listed in Section 7.2.

6. Calibration and Validation:

Direct in-situ measurements of latent and sensible heat fluxes are limited within CYGNSS's orbit and often only available during field campaigns or on a limited number of research buoys. Though these comparisons may be available for future versions of this product, for now, we have been able to use estimates from buoy data that matchup with CYGNSS observations. While these buoys may not measure the fluxes directly, they do measure wind speeds, temperature, and humidity, which can be inputted into the same COARE algorithm used to estimate the fluxes for the L2 CYGNSS fluxes (Crespo et al. 2019).

Buoy data was obtained from the following buoy networks: Kuroshio Extension Observatory (KEO), National Data Buoy Center (NDBC), Ocean Sustained Interdisciplinary Timeseries Environment observation System (OceanSITES), Prediction and Research Moored Array in the Tropical Atlantic (PIRATA), Research Moored Array for African-Asian-Australian Monsoon Analysis and Prediction (RAMA), and the Tropical Atmosphere Ocean Array (TAO).

For these comparisons, any values from the CYGNSS Surface Heat Flux Product that had a quality flag associated with them were removed. The remaining specular points were then used to compare the fluxes estimated from the buoys, with the resulting comparison in Figure 5. As shown in Fig. 5, at lower flux values, the CYGNSS surface heat fluxes compare well with the buoy data and are along the one-to-one line. While the density plot shows a decent width (at least for LHF) around this line, overall, most of the fluxes from CYGNSS are in agreement and validate well with the buoy data.

However, as the fluxes increase, there is greater scatter and disagreement between CYGNSS and the buoy data. For the LHF results, while CYGNSS overestimated some of the fluxes, it more often underestimated the fluxes, whereas it consistently underestimated higher SHF values. As a result, the overall RMSD for the FDS version of LHF was almost 38 W/m^2, while the FDS version of SHF RMSD was 8.5 W/m^2. The YSLF versions of these products saw higher RMSD values, especially LHF with an RMSD of 50.7 W/m^2. Given that there were nearly 75% fewer sample points between the YSLF and FDS products, this likely explains these drastic differences.

The differences observed at higher flux values likely came from uncertainties in the L2 CYGNSS wind speed, as there have been known errors at higher wind speeds. Additionally, there may be other errors from MERRA-2 that were not factored in, such as errors related to precipitation. Granted, the number of comparisons at the higher flux values were limited, which may have resulted in the observed scatter. Future releases of the CYGNSS L2 wind speeds are expected

to reduce these residual errors, while further investigation is also needed to assess and address the introduction of uncertainties from MERRA-2 in future product releases.

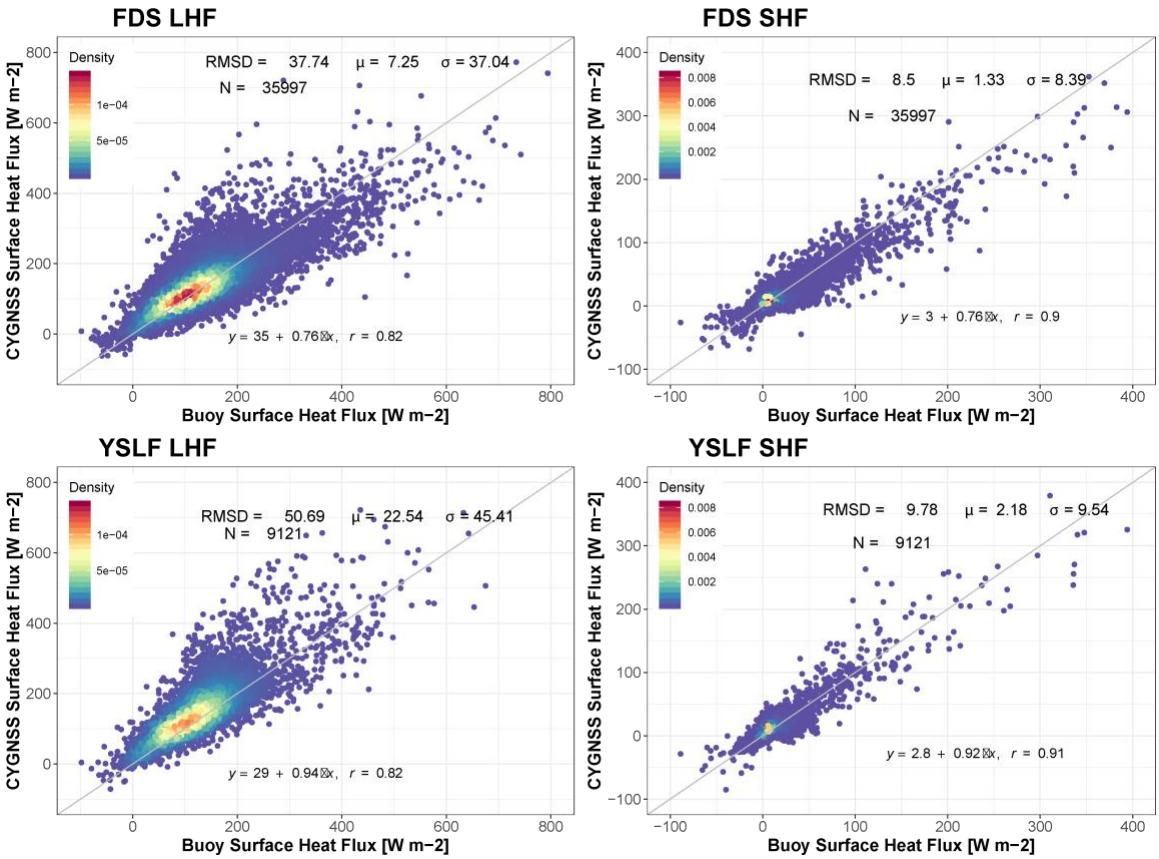

Figure 5: CYGNSS surface heat flux comparisons (y-axis) compared to flux estimates from buoys (x-axis). Top row: CYGNSS LHF and SHF estimates using the FDS wind speed product. Bottom Row: CYGNSS LHF and SHF estimates using the YSLF wind speed product. Left: Latent heat flux. Right: Sensible heat flux.

Despite these likely errors and uncertainties, the fluxes from the CYGNSS Surface Heat Flux product compare well with the ground truth from the buoy data. Future releases hope to include comparisons and validation with various field campaigns (e.g. PISTON, CAMP2Ex) as well more buoy data, especially at higher flux estimates.

7. Dataset Description:

This dataset is being distributed in netCDF-4 format using internal compression (more computationally efficient compared to external compression such as gzip) and adhering to CF v1.6 and ISO-8601 conventions. Each file is unique to a particular calendar day of a year and consists of one complete orbital revolution (assuming no data gaps).

The file naming convention is cyg.ddmi.sYYYYMMDD-HHMMSS-eYYYYMMDD-HHMMSS.l2.surface-flux-cdr.aAA.dVV.nc, where:

cyg = CYGNSS, which is the mission and platform source of the dataset.
ddmi = Delay Doppler Mapping Instrument.
sYYYYMMDD = the year, month and day of the starting point of the first data in the file.
HHMMSS = Hour, minutes and seconds (respectively) of date/time stamp.
eYYYYMMDD = the year, month and day of the ending point of the last data in the file.
l2 = Level 2 processing.
surface-flux-cdr = surface flux dataset (climate data record version).
aAA = Algorithm version, where AA is the numerical algorithm version identifier. E.g., "a10" = Algorithm Version 1.0. Note: the Algorithm version is numerically de-coupled from the Dataset Version (see below).
dVV = Dataset version, where VV is the numerical dataset version identifier. E.g., "d10" = Dataset Version 1.0. Note: the Dataset version is numerically de-coupled from the Algorithm Version (see above).
.nc = the file extension indicating the usage of netCDF data formatting

The date and time represented by the file name is with respect to GMT (UTC). Greater precision of the start and stop times is available in the netCDF global attributes.

7.2 Variable Types

Table 2. Dataset Variable Description

Name	Data Type	Missing Value	Description
sample	long	N/A	The netCDF coordinate variable associated with the sample dimension, which enumerates the zero-justified index range of the DDM time instants contained in the file.
sample_time	double	-9999.f	The mean UTC timestamp of the DDMs that were utilized to derive wind_speed from the original CYGNSS L2 data files. Note that the DDM sampling period is not synchronized with the UTC change of

			second so sample_time can occur at any time relative to the UTC change of second.
spacecraft_id	short	-9999s	The CCSDS spacecraft identifier:\n\t0xF7 (247): CYGNSS 1\n\t0xF9 (249): CYGNSS 2\n\t0x2B (43): CYGNSS 3\n\t0x2C (44): CYGNSS 4\n\t0x2F (47): CYGNSS 5\n\t0x36 (54): CYGNSS 6\n\t0x37 (55): CYGNSS 7\n\t0x49 (73): CYGNSS 8\n\t0x00 (0): end to end simulator\n\t0x0E (14): engineering model\n\t0x0D (15): default\n\t0xFF (255): unknown\n
spacecraft_num	byte	-99b	The CYGNSS spacecraft number: Ranges from 1 through 8 and 99. 1 through 8 are on-orbit spacecraft. 99 is the CYGNSS end-to-end simulator.
prn_code	byte	-99b	The PRN code of the GPS signal associated with the DDMs utilized to derive heat fluxes. Ranges from 0 to 32. 0 = reflectometry channel idle. 1 to 32 represent a PRN code.
lat	float	N/A	The mean of the specular point latitudes of the DDMs that were utilized to derive wind_speed, degrees North.
lon	float	N/A	The mean of the specular point longitudes of the DDMs that were utilized to derive wind_speed, degrees East.

air_density	float	-9999.f	Air density at surface received from the MERRA-2 variable \'RHOA\'.
effective_surface_humidity	float	-9999.f	"Effective surface specific humidity received from the MERRA-2 variable \'QSH\'.
specific_humidity	float	-9999.f	10 meter specific humidityreceived from the MERRA-2 variable \'QV10M\'.
surface_pressure	float	-9999.f	Surface pressure received from the MERRA-2 variable \'PS\'
air_temperature	float	-9999.f	10 meter air temperature received from the MERRA-2 variable \'T10M\'
lhf	float	-9999.f	The latent heat flux estimates at each specular point using the CYGNSS Level-2 wind_speed FDS minimum variance product.
shf	float	-9999.f	The sensible heat flux estimates at each specularpoint using the CYGNSS Level-2 wind_speed FDS minimum variance product.
lhf_yslf	float	-9999.f	The latent heat flux estimates at each specular point using the CYGNSS Level-2 YSLF NBRCS product.
shf_yslf	float	-9999.f	The sensible heat flux estimates at each specular point using the CYGNSS Level-2 YSLF NBRCS product.
lhf_uncertainty	float	-9999.f	Standard deviation of the additive latent heat

			flux error, based on known and reported uncertainties from CYGNSS L2 FDS winds, and MERRA-2 temperature and humidity. Dependent on lhf, in W m-2.
shf_uncertainty	float	-9999.f	Standard deviation of the additive sensible heat flux error, based on known and reported uncertainties from CYGNSS L2 FDS winds, and MERRA-2 temperature and humidity. Dependent on shf, in W m-2.
lhf_uncertainty_yslf	float	-9999.f	Standard deviation of the additive latent heat flux error, based on known and reported uncertainties from CYGNSS L2 YSLF winds, and MERRA-2 temperature and humidity. Dependent on lhf_YSLF, in W m-2.
shf_uncertainty_yslf	float	-9999.f	Standard deviation of the additive sensible heat flux error, based on known and reported uncertainties from CYGNSS L2 YSLF winds, and MERRA-2 temperature and humidity. Dependent on shf_yslf, in W m-2.
cygnss_l2_sample_index	long	N/A	A sample index for the corresponding CYGNSS L2 sample index used for deriving the heat fluxes. This can be used with \'source\' to look up the CYGNSS L2 data and metadata.
quality_flags	short	-9999s	See section 7.3 below.

7.3 Bit by Bit Description of Quality Flag Variable

The following tables describes all the bits in the quality flag variable.

Bit Number (0=LSB)	Flag Value (2^bit#)	Bit Name	Meaning when bit is 1 (1 means bit has been set; 0 means unset).
0	1	poor_overall_quality	If any one of the following flags are set then poor_overall_quality will be set: low_quality_gps_ant_knowledge OR low_range_corrected_gain OR cygnss_l2_fatal_flag OR low_FDS_wind_speed OR low_yslf_nbrcs_wind_speed OR high_FDS_wind_speed OR high_yslf_nbrcs_wind_speed
1	2	spare_1	Always zero
2	4	low_range_corrected_gain	Range corrected gain is less than 3.
3	8	ascending_satellite	Satellite is on the ascending node of the orbit (subsatellite point latitude is increasing).
4	16	cygnss_l2_fatal_flag	CYGNSS Level-2 Fully Developed Seas (FDS) sample flag is set to fatal; data is discarded for FDS wind speed.
5	32	low_general_wind_speed	CYGNSS Level-2 FDS wind speed < 0 m/s.
6	64	low_yslf_nbrcs_wind_speed	CYGNSS Level-2 YSLF NBRCS wind speed < 0 m/s.
7	128	high_general_wind_speed	CYGNSS Level-2 FDS wind speed > 25 m/s.
8	256	high_yslf_nbrcs_wind_speed	CYGNSS Level-2 YSLF NBRCS wind speed > 25 m/s.
9	512	cygnss_l2_yslf_fatal_flag	CYGNSS Level-2 YSLF sample flag is set to fatal

7.4 Grid Description

Given that LHF and SHF are calculated at every specular point observed by CYGNSS, the spatial distribution of the CYGNSS Heat Flux Product is the same as the Level-2 CYGNSS CDR V1.0 Wind Speed Product (see References, section

10, for details). As discussed in Section 4.1, each specular point is 25 km wide; at the beginning of the mission, each spacecraft was observing up to four specular points per second (32 per second for the entire constellation). Beginning in July 2019, the sampling was reduced from once per second to once every half second, reducing along-track beam smearing and now resulting in up to 64 wind speed observations per second for the entire constellation. The reflected signal from the GPS satellite will remain within CYGNSS's antenna view pattern, allowing for long swaths of continuous specular point observations; the length of these swaths is not consistent.

Though CYGNSS's orbit reaches the 35th parallel in both hemispheres, it can consistently make observations up to 38th parallel, allowing it observe non-tropical systems (Crespo et al. 2017, 2019). On average, CYGNSS has a median revisit time of just under 3 hours and a mean of around 7 hours. However, this is not consistent across its orbit. Near the edge of its orbit, CYGNSS's revisit time is much longer, though can feature many observations within the span of a few hours; revisit times are much shorter near the equator (Park et al. 2019).

7.5 Related Products

All related data products are referenced here:
https://podaac.jpl.nasa.gov/datasetlist?ids=Collections&values=CYGNSS

8. Data Access:

Obtaining Data and Documentation:

Note: the documentation (/doc) are located one directory level above the data directories.

MD5 checksum files are also available for all datasets in the data directories to assist you in verifying the integrity of each data file/granule. To learn more about MD5 checksums, you may visit: https://en.wikipedia.org/wiki/MD5

The PO.DAAC Drive HTTPS service is now available to access all data. To use PO.DAAC Drive, you may visit: https://podaac-tools.jpl.nasa.gov/drive/

For information on how to cite this data in presentations or publications, please read:
https://podaac.jpl.nasa.gov/CitingPODAAC

For general news, announcements, and information on this and all other ocean and sea ice datasets available at PO.DAAC, please visit the PO.DAAC web portal: https://podaac.jpl.nasa.gov/

Contact Information:

Questions and comments should be directed to the Physical Oceanography Distributed Active Archive Center (PO.DAAC) at the NASA Jet Propulsion Laboratory (JPL). Please note that email is always the preferred method of communication, but Forum is highly recommended as a first point of entry to address Frequently Asked Questions.

E-Mail: podaac@podaac.jpl.nasa.gov

WWW: https://podaac.jpl.nasa.gov/forum

Mail: PO.DAAC User Services Office

Jet Propulsion Laboratory

M/S T1721-202

4800 Oak Grove Drive

Pasadena, CA 91109

9. Read Software:

Sample L2B netCDF software readers are currently available in IDL, MATLAB, R and Python at the following location: https://podaac-tools.jpl.nasa.gov/drive/files/common/sw/generic_nc_readers

10. References:

Beljaars, A. C. M., and A. A. M. Holtslag, 1991: Flux parameterization over land surfaces for atmospheric models. *J. Appl. Meteor*., **30**, 327–341.

Clarizia, M. P., and C. S. Ruf, “Wind Speed Retrieval Algorithm for the Cyclone Global Navigation Satellite System (CYGNSS) Mission,” IEEE Trans Geosci. Remote Sens., doi:10.1109/TGRS.2016.2541343, 2016.

Crespo, J.A., D.J. Posselt, C.M. Naud, and C.D. Bussy-Virat, 2017: Assessing CYGNSS's Potential to Observe Extratropical Fronts and Cyclones. *J. Appl. Meteorol. Climatol.*, **56**, 2027-2034, doi:10.1175/JAMC-D-17-0050.1.

Crespo, J. A., D. J. Posselt, and S. Asharaf, 2019: CYGNSS Surface Heat Flux Product Development. *Remote Sens.*, **11**, 2294, doi: 10.3390/rs11192294.

CYGNSS. 2020. CYGNSS Level 2 Climate Data Record Version 1.0. Ver. 1.0. PO.DAAC, CA, USA. Dataset accessed 2020-05-23 at https://doi.org/10.5067/CYGNS-L2C10.

Edson, J., V. Jampana, R. Weller, S. Bigorre, A. Plueddemann, C. Fairall, S. Miller, L. Mahrt, D. Vickers, and H. Hersbach, 2013: On the exchange of momentum over the open ocean, *J. Phys. Oceanogr.*, **43**, 1589–1610, doi:10.1175/JPO-D-12-0173.1.

Fairall, C. W., E. F. Bradley, D. P. Rogers, J. B. Edson, and G. S. Young, 1996: Bulk Parameterization of Air–sea Fluxes for Tropical Ocean–Global Atmosphere Coupled Ocean—Atmosphere Response Experiment. *J. Geophys. Res.*, **101**, 3747–3764.

Fairall, C. W., A. B. White, J. B. Edson, and J. E. Hare, 1997: Integrated shipboard measurements of the marine boundary layer. *J. Atmos. Oceanic Technol.*, **14**, 338-359.

Gelaro, R., W. McCarty, M.J. Suárez, R. Todling, A. Molod, L. Takacs, C.A. Randles, A. Darmenov, M.G. Bosilovich, R. Reichle, K. Wargan, L. Coy, R. Cullather, C. Draper, S. Akella, V. Buchard, A. Conaty, A.M. da Silva, W. Gu, G. Kim, R. Koster, R. Lucchesi, D. Merkova, J.E. Nielsen, G. Partyka, S. Pawson, W. Putman, M. Rienecker, S.D. Schubert, M. Sienkiewicz, and B. Zhao, 2017: The Modern-Era Retrospective Analysis for Research and Applications, Version 2 (MERRA-2).The Modern-Era Retrospective Analysis for Research and Applications, Version 2 (MERRA-2). *J. Climate,* **30**, 5419–5454, https://doi.org/10.1175/JCLI-D-16-0758.1

Gleason, S., “Remote Sensing of Ocean, Ice and Land Surfaces Using Bistatically Scattered GNSS Signals from Low Earth Orbit,” Ph.D. diss., University of Surrey, UK, 213 pp, 2006.

Park, J., J.T. Johnson, Y. Yi, and A.J. O’Brien, 2019: Using “Rapid Revisit” CYGNSS Wind Speed Measurements to Detect Convective Activity. *J. Sel. Top. Appl. Earth Observ. Remote Sens.*, **12**, 98-106 doi: 10.1109/JSTARS.2018.2848267.

Richter, D. H., and D. P. Stern, 2014: Evidence of spray-mediated air-sea enthalpy flux within tropical cyclones, *Geophys. Res. Lett.*, **41**, 2997–3003, doi:10.1002/2014GL059746.

Ruf, C., P. Chang, M.P. Clarizia, S. Gleason, Z. Jelenak, J. Murray, M. Morris, S. Musko, D. Posselt, D. Provost, D. Starkenburg, V. Zavorotny, CYGNSS Handbook, Ann Arbor, MI, Michigan Pub., ISBN 978-1-60785-380-0, 154 pp, 1 Apr 2016.

11. Acronyms:

COARE: Coupled Ocean-Atmosphere Response Experiment
CYGNSS: CYclone Global Navigation Satellite System
CF: NetCDF Climate and Forecast (CF) Metadata Convention
DDM: Delay Doppler Map
DDMI: Delay Doppler Mapping Instrument
FDS: Fully Developed Seas
GMF: Geophysical Model Function
GMT: Greenwich Mean Time (also known as Zulu or UTC time)
IDL: Interactive Data Language
JPL: Jet Propulsion Laboratory
KEO: Kuroshio Extension Observatory
LHF: Latent Heat Flux
LSB: Least Significant Bit
MD5: Message-Digest Algorithm
MERRA: Modern-Era Retrospective analysis for Research and Applications
NASA: National Aeronautics and Space Administration
NDBC: National Data Buoy Center
NetCDF: Network Common Data Form
NOAA: National Oceanic and Atmospheric Administration
OceanSITES: Ocean Sustained Interdisciplinary Timeseries Environment observation System
OPeNDAP: Open-source Project for a Network Data Access Protocol
PIRATA: Prediction and Research Moored Array in the Tropical Atlantic
PRN: Pseudorandom Noise Number
PO.DAAC: Physical Oceanography Distributed Active Archive Center
RAMA: Research Moored Array for African-Asian-Australian Monsoon Analysis and Prediction
RMSD: Root Mean Square Difference
SHF: Sensible Heat Flux
TAO: Tropical Atmosphere Ocean Array
YSLF: Young Seas with Limited Fetch

12. Document History

Document Last Modified Draft Date:

6 October 2020

Document Review Date:

21 September 2020

Citation:

A majority of the document material was provided by the CYGNSS Handbook (Ruf et al. 2016) with primary dataset inputs provided by Juan Crespo and Derek Posselt. Dr. Shakeel Asharaf produced and provided the buoy match-ups shown in Figure 3. David Moroni was responsible for all remaining inputs, the overall document templatization and curation.

Citation of the PO.DAAC datasets should follow PO.DAAC general dataset citation guidelines as mentioned here: https://podaac.jpl.nasa.gov/CitingPODAAC.

To cite the use of the Level 2 dataset in a publication (i.e., presentation or manuscript), please use the following template:

CYGNSS. 2020. CYGNSS Level 2 Surface Flux Climate Data Record Version 1.0. PO.DAAC, CA, USA. Dataset accessed [YYYY-MM-DD] at https://doi.org/10.5067/CYGNS-C2H10.

Document Location:

The direct PO.DAAC Drive Link for CYGNSS Level 2 documentation is available here: https://podaac-tools.jpl.nasa.gov/drive/files/allData/cygnss/L2/docs